International Journal of Innovation, Creativity and Change. www.ijicc.net
Volume 8, Issue 5, 2019

# Development of an SRM-based Drive for Built-in Automotive Vacuum Cleaners

**Jaehyuck Kim,** Wonkwang University, Email: jaehkim@wku.ac.kr

The paper describes the design and control of a switched reluctance motor (SRM) and drive system for built-in automotive vacuum cleaners. As the popularity of outdoor activities and recreation has increased, the automobile industry has expanded technology to enhance vehicle convenience and vacuum cleaners with built-in automobiles have been introduced. The conventional DC motors in vacuum cleaning systems have several disadvantages such as maintenance cost and life of the commutator-brush structure. The SRM is a good alternative to existing DC motors due to its high-speed capability, long life, low maintenance costs and high efficiency. The prototype SRM drive is designed and built to verify its use in a built-in automotive vacuum cleaner system. Dynamic simulation is performed to determine the optimum switching angle for maximum efficiency and minimum torque ripple. Load tests, noise measurements and suction tests are also performed.

**Key words:** *Built-in car vacuum cleaners, Motor drive, Switched reluctance motor, Variable speed drive.*

## Introduction

As the outdoor activities and various leisure activities of family units are increasing, industries related to vehicle convenience and smart automobile technology are increasing. In this regard, there is a growing need for a built-in cleaner for vehicles. A few automobile makers have applied t built-in car vacuum cleaners to their new minivan line-ups. However, the DC motor of the brush-commutator type structure applied to conventional vacuum cleaners has disadvantages of low suction force, mechanical brush wear and a carbon dust problem. Alternative motors should be developed to alleviate those problems.

A switched reluctance motor (SRM) is a typical non-rare-earth motor and its application is increasing in many industrial fields in recent years. SRM is simple and robust in structure because it does not have permanent magnets nor windings in the rotor and it has simple concentrated windings in the stator (Krishnan, 2001). Therefore, production cost is low compared to other motors. Also, it has excellent durability and reliability due to its robust structure and it has high speed capability and high starting torque.

This paper presents the design, fabrication, dynamic simulation and experimental results of a prototype SRM for use in built-in automotive vacuum cleaners. The proposed motor drive system can improve both durability and suction power by using SRM instead of conventional DC motor.

## Motor Development

The structure of the two-phase 4/2 SRM considering the required output power, speed, and load conditions of the built-in vacuum cleaners for vehicles is shown in Figure 1 below and the design specifications are as shown in Table 1 below. For t same performance evaluation of the SRM compared with the DC motor, which is currently applied in most of the vacuum cleaners, design criteria were selected considering the capacity, driving speed and load condition of the DC motor-based vacuum cleaners.

**Table 1:** Specification of the prototype 4/2 SRM

| Parameter | Value | Unit |
|---|---|---|
| Rated power | 150 | W |
| Rated speed | 32,000 | r/min |
| Rated torque | 0.0045 | N-m |
| Maximum efficiency | 65 | % |

The SRM basically determines the magnitude of the constant and the possible pole angle depending on the combination of poles of the stator and rotor. There are many different topologies for SRM but two-phase SRM is most suitable due to self-starting capability and less core loss compared with other multiphase SRMs. Based on the combination of stator and rotor poles, several combinations of stator and rotor poles have been presented in Table 2 below. Considering magnetic capability, efficiency (iron loss) and manufacturing cost, a 4 or 2 pole combination is the best option and therefore, the 4/2 SRM has been selected in consideration of manufacturing cost and efficiency.

**Table 2:** Stator and rotor pole combinations for the two-phase SRM

| No. of stator poles | No. of rotor poles | Stoke angle | No. of strokes per revolution |
|---|---|---|---|
| 4 | 2 | 90° | 4 |
| 4 | 6 | 30° | 12 |
| 6 | 3 | 60° | 6 |
| 6 | 9 | 20° | 18 |
| 8 | 4 | 45° | 8 |

**Figure 1.** Two-phase 4/2 Switched reluctance motor for high speed application

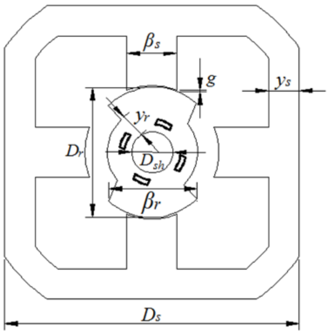


The design parameters and definitions of SRM are shown in Fig. 1 and Table 3.

**Table 3:** Specification of the prototype 4/2 SRM

| Parameter | Description | Unit |
|---|---|---|
| $D_s$ | Stator outer dimension | mm |
| $D_r$ | Rotor outer diameter | mm |
| $D_{sh}$ | Shaft Diameter | mm |
| $y_s$ | Stator yoke thickness | mm |
| $y_r$ | Rotor yoke thickness | mm |
| $\beta_s$ | Stator pole arc | ° |
| $\beta_r$ | Rotor pole arc | ° |
| $G$ | Airgap length | mm |

The output power equation of the SRM is given by Eq (1) where $k_d$ is the duty ratio, $k_e$ the is efficiency of the motor, $B$ is the magnetic flux density in stator-rotor alignment, $A_s$ is the electrical load, $D$ is the outer diameter of the rotor, $L$ is the core length of the stator, and $\omega_r$ is the rotor angular speed.

$$P = k_d k_e k_1 k_2 B A_s D^2 L \omega_r \qquad (1)$$

$$\left(k_1 = \frac{\pi^2}{120}, \qquad k_2 = 1 - \frac{1}{\sigma_s \sigma_u}\right)$$

Using Eq. (1), the electromagnetic torque of the SRM can be derived as

$$T_e = k_d k_e k_2 k_3 B A_s D^2 L \qquad (2)$$

where $k_3 = \frac{\pi}{4}$.

It is important to derive accurate magnetic (inductance) and torque characteristics for various excitation currents in motor design and control. Inductance and torque data according to rotor position were obtained for various excitation currents through finite element analysis program. Fig. 2 and Fig. 3 below represent the inductance profiles and the torque profiles for 4/2 two-phase SRM respectively. The magnetic properties of the rotor-current-inductance and the torque characteristics of the rotor-current-torque obtained through finite element analysis are used for simulation and control angle tuning during high speed rated speed operation.

**Figure 2.** Inductance profiles of the 24V two-phase 4/2 SRM

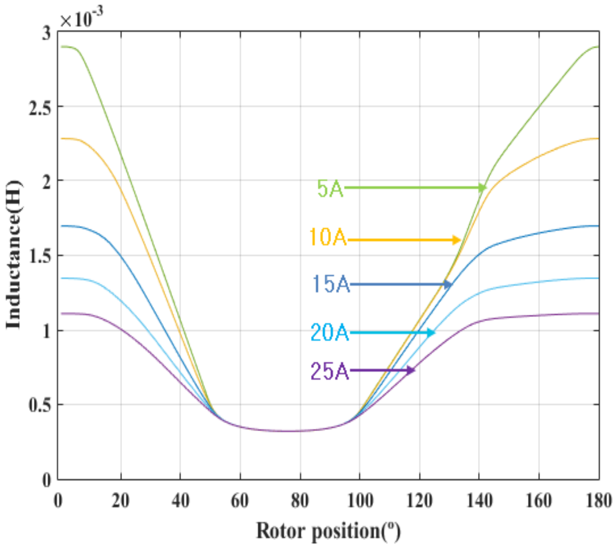

**Figure 3.** Torque profiles of the 24V two-phase 4/2 SRM

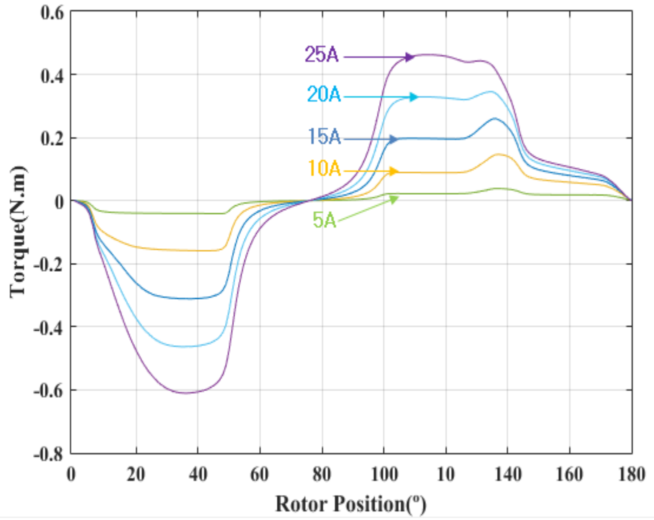


### Converter Development

**Figure 4.** Drive circuit (Asymmetric half bridge converter) for two-phase SRM

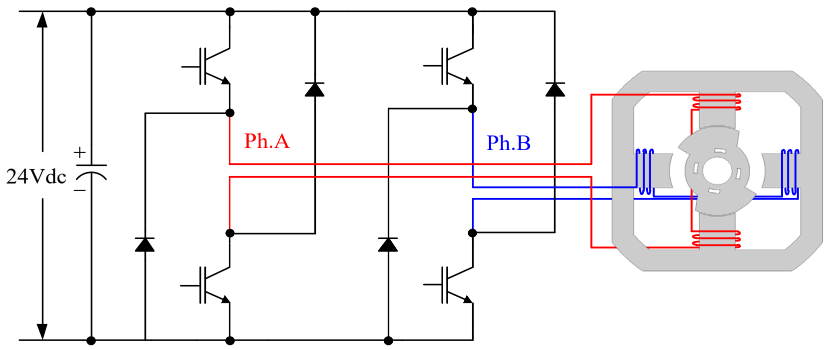


The SRM has many advantages over inverter-driven three-phase motors (BLDC, PMSM). Fig. 4 above shows the schematic of the drive circuit for two-phase SRM. As shown in the figure, the conventional three-phase motor has no independence between phases and there is a risk of shoot-through failure between the high-side and low-side switches of the inverter bridge. In case of SRM drive however each phase winding is located between the high-side and low-side switches, so there is no shoot-through failure at all. This is one of the great advantages that SRM provides with excellent reliability.

Since the generation of SRM reluctance torque is independent of the direction of the current and the mutual coupling between the phases is very small. Hence, various types of converter configurations are possible for SRM unlike inverters in three-phase motors. Among many converter topologies, the asymmetric half bridge converter as shown in Figure 4 above is most commonly used in consideration of control performance and system stability. Inexpensive converters that require only one switching element in one phase are cost-effective and economical (Jeon, Kim, & Lee, 2016; Lee, Kim, & Jeon, 2016; Lim, Jung, Kim, & Kim, 2001), but are not suitable for in-vehicle power supplies with low input voltage. The asymmetric half bridge converter for two-phase SRM consists of four switching elements and four diodes. Each phase can be controlled independently and does not affect other phases when one phase fails.

Fig 5 below shows operation modes of the asymmetric half-bridge converter (Effendi, Rahman, & Hendrawan, 2017; Koh, Hun Oh, & Park, 2016; Lee, Lin, & Chang, 2018; Mahmood & Chung, 2017; Marat, Assem, Bakhytzhan, & Peter, 2016). There are three (positive, zero, negative) modes according to the input voltage state transferred to one phase according to the conduction state of the switching element and diode of each phase which correspond to the non-magnetizing mode.

**Figure 5.** Operation modes of asymmetric bridge converter for two-phase SRM

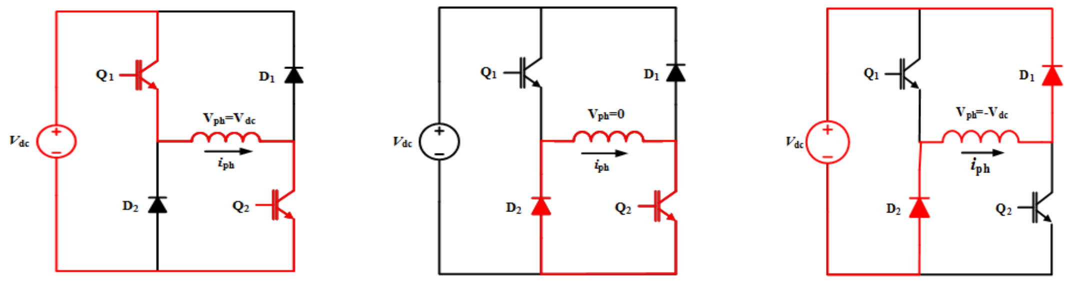


(a) Positive voltage mode (b) Zero Voltage Mode (c) Negative voltage mode

### Simulation Results

In order to verify the dynamic characteristics and performance of the two-phase 4/2 SRM drive and to tune the controller parameters, dynamic simulation was carried out follows. The two-phase SRM drive system is modelled using Matlab / Simulink and the mathematical model of the two-phase SRM for the simulation model is described below. The voltage applied to one phase winding of the SRM is equal to the sum of the voltage drop due to the resistance and the change in magnetic flux with time.

$$v = R_s i + \frac{d\lambda(\theta, i)}{dt}$$

$$= R_s i + \frac{dL(\theta, i)}{dt}$$

$$= R_s i + L(\theta, i)\frac{di}{dt} + i\frac{d\theta}{dt}\frac{dL(\theta,i)}{d\theta} \qquad (3)$$

In Equation (3), the terminal voltage of the phase winding, the current flowing through the phase winding, the flux linkage, the phase resistance, the phase inductance, the rotor position, and the angular velocity of the rotor are the context. The voltage drop due to the inductance and the back electromotive force indicate the voltage drop due to the inductance.

Generally, the torque of the SRM phase can be expressed as follows.

$$T_e = \frac{i^2}{2}\frac{dL(\theta,i)}{d\theta} \qquad (4)$$

In addition, the equation of rotational motion between the torque and the rotor speed is given by

$$T_e = B\omega + J\frac{d\omega}{dt} + T_L \qquad (5)$$

The friction coefficient, the inertia moment and the load torque respectively. A block diagram of the mathematical model of the electrical system and the mechanical system of the two-phase SRM using mathematical models from Equations (3) to (5) is shown in Figure 6 below.

**Figure 6.** Block diagram of a two-phase SRM for simulation modelling

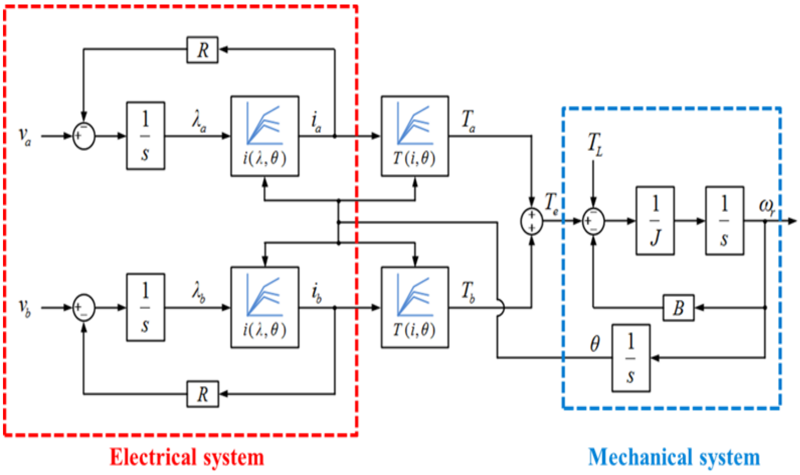


The simulation was performed under the conditions of rated speed 32,000rpm, rated torque 0.045N-m and PWM switching frequency 20kH, as shown in Table 3, and the resulting simulation waveform is shown in Figure 7 below.

**Figure 7.** Simulation model of two-phase SRM drive system implemented by Matlab / Simulink

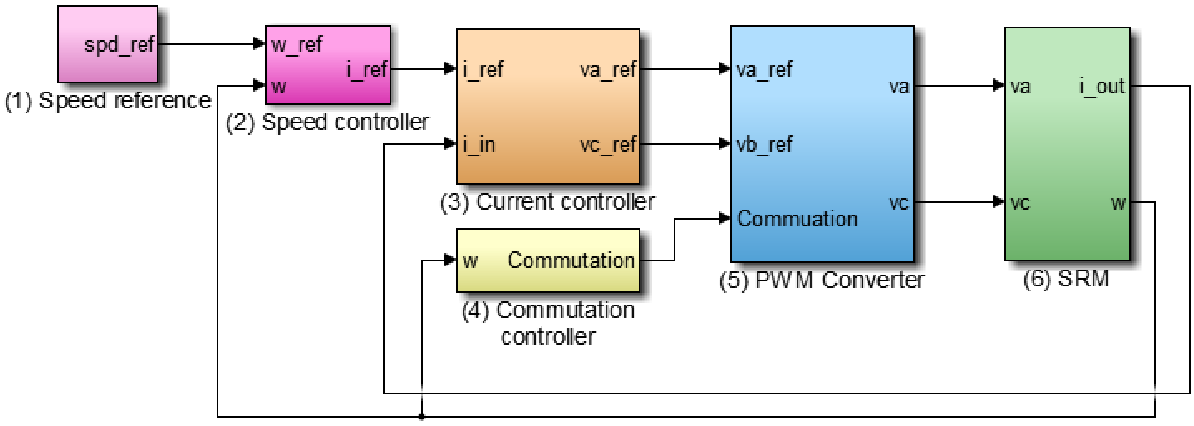


**Figure 8.** Simulated waveforms of phase voltages, phase currents, and torque when the SRM is rotating at 32,000 rpm.

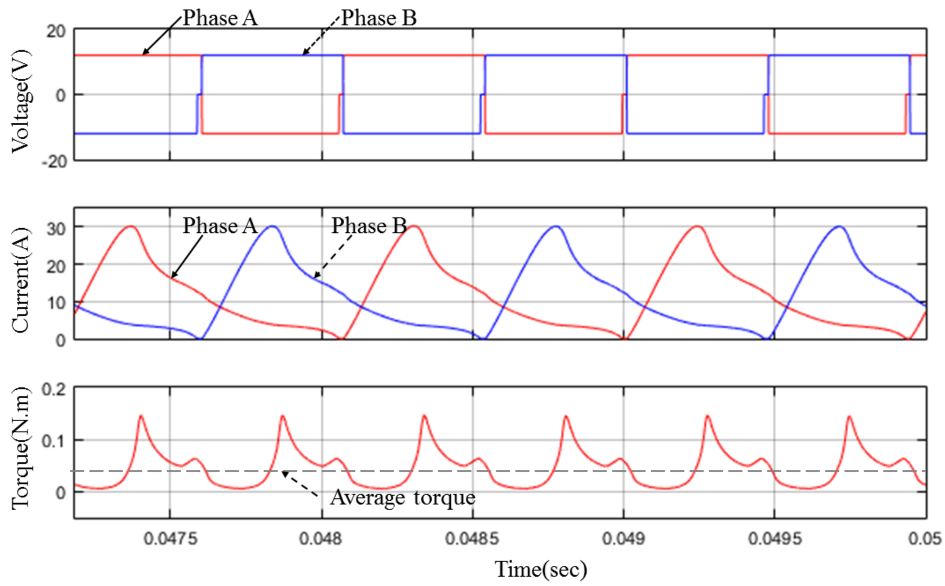


## Experimental Results

**Figure 9.** Experiment setup for load test

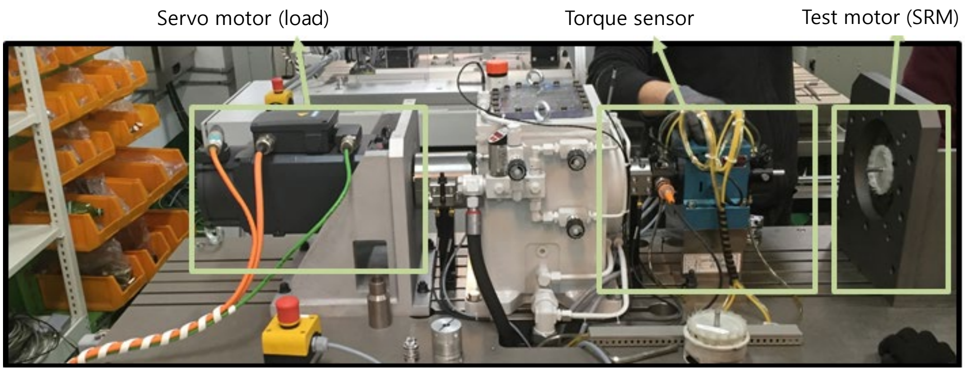

**Figure 10.** Measured waveforms of phase voltage and phase currents

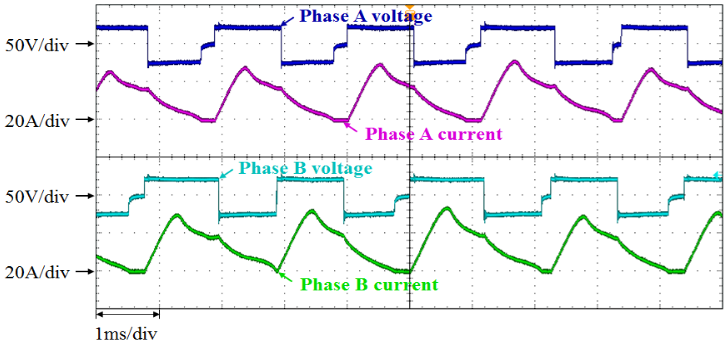


In order to verify the capability of the cleaner motor for the two-phase 4/2 SRM manufactured, the suction force test was performed through the motor suction force testing device (Ahmadi, 2017; Koh, Hun Oh, & Park, 2016). As shown in Table 4 below, suction power was measured at each different load and orifice condition. At this time, the suction efficiency of the vacuum cleaner is 40%, which is 5% higher than the suction efficiency of 39% measured when the conventional DC motor is installed.

**Table 4:** Suction power test results

| Orifice Dia. [mm] | Current [A] | Input Power [W] | Air Flow [ /sec] | Suction Power [W] | Efficiency [%] |
|---|---|---|---|---|---|
| 22 | 13.7 | 322 | 20.84 | 107.24 | 33.31 |
| 21 | 14.56 | 341 | 20.99 | 132.73 | 38.92 |
| 20 | 14.58 | 341 | 19.85 | 136.54 | 40.04 |
| 19 | 14.26 | 333 | 18.52 | 136.45 | 40.98 |
| 18 | 14.29 | 334 | 17.1 | 133.44 | 39.95 |
| 17 | 13.84 | 324 | 15.62 | 127.92 | 39.48 |

**Conclusions**

In order to develop high speed SRM for built-in automotive vacuum cleaners, a motor and controller were designed and fabricated. A load test as well as a suction test were carried out under rated speed and rated load condition. A suction power test was also carried out to verify whether there was sufficient output power as required by the vacuum cleaner and based on the simulation and test results the results confirm that they are competitive enough for built-in car vacuum cleaners. The competitiveness of the SRM in the field of built-in cleaners for automobiles was also confirmed by simulating and testing the developed drive system.

**Acknowledgement**

This paper was supported by Wonkwang University in 2018.

**REFERENCES**

Ahmadi, (2017). The feasibility study on trapping experiments with lights in Barito river of Indonesia. *Journal of Advances in Technology and Engineering Research*, *3*(6), 235-243.

Effendi, M. S., Rahman, N., & Hendrawan, A. (2017). The use of solar collector as preheater and condensate pipe as heat recovery in basin solar still to increase efficiency. *International Journal of Technology and Engineering Studies, 3*(6), 264-273.

Jeon, W.R., Kim, S. P., & Lee, J. H. (2016). Numerical analysis and optimum design for the vacuum jacket valve. *Journal of Advances in Technology and Engineering Research, 2*(1), 1-5.

Kim, J., & Krishnan, R. (2008). High efficiency single-pulse controlled switched reluctance motor drive for high speed (48k rpm) application: Analysis, design, and experimental verification. In *2008 IEEE Industry Applications Society Annual Meeting (pp. 1-8)*, Alberta, Canada: IEEE.

Koh, R., Hun Oh, Y., & Park, D. (2016). A study on formation of saltwater-freshwater interface and upconing in coastal aquifers based on experiments with hydraulic models. *Journal of Advances in Technology and Engineering Studies, 2*(5), 134-139.

Krishnan, R. (2001). *Switched reluctance motor drives. Industrial electronics series*. New York, NY: CRC Press.

Lee, C.Y., Lin, J. Y., & Chang. R. I. (2018). Improve Quality and Efficiency of Textile Process using Data-driven Machine Learning in Industry 4.0. *International Journal of Technology and Engineering Studies, 4*(1), 64-76.

Lee, J. H., Kim, S. P., & Jeon, R. W. (2016). Optimal design for adiabatic pipes using vacuum at cryogenic temperatures. *Journal of Advances in Technology and Engineering Research*, *2*(2), 6-11.

Lim, J. Y. (2002). Household appliances use cases of SRM. *KIPE Magazine*, *7*(4), 27-37.

Lim, J. Y., Jung, Y. C., Kim, S.Y., & Kim, J. C. (2001). Single Phase Switched Reluctance Motor for Vacuum Cleaner. In *ISIE 2001Proceedings (pp. 1393-1400)*, Pusan, South Korea: IEEE.

Mahmood, A., & Chung, L. L. E. (2017). Experimental modelling of a reinforcement theoretical model on peaty soils. *International Journal of Applied and Physical Sciences, 3*(3), 75-84.

Marat, K., Assem, Y., Bakhytzhan, M., & Peter, K. (2016). Theoretical and experimental researches on development of new construction of wind-driven generator with flux concentrator. *Journal of Advances in Technology and Engineering Research*, *2*(3), 100-104.